

Impact of Flux Barriers Type and Parameterization in Reluctance Machine Torque Optimization

Christophe De Gréef¹, Virginie Kluykens¹, François Henrotte^{1,2}, Christophe Geuzaine², Bruno Dehez¹

¹*Institute of Mechanics, Materials and Civil Engineering (IMMC)*

Université catholique de Louvain (UCLouvain), Louvain-la-Neuve, Belgium

{christophe.degreeef, virginie.kluykens, francois.henrotte, bruno.dehez}@uclouvain.be

²*Department of Electrical Engineering and Computer Science, Montefiore Institute*

Université de Liège (ULiège), Liège, Belgium

{francois.henrotte, cgeuzaine}@uliege.be

Abstract—This paper analyzes the impact of the flux barriers (FB) type and their parameterization on the torque optimization of synchronous reluctance machines. Four different types are considered: rectangular FB, round FB, hyperbolic FB, and finally Joukowski FB, which follow the natural flux lines in a solid rotor. A parameterization that simplifies the non-overlapping constraints is introduced, and, for each of these types, the number of parameters is discussed. A multi-objective optimization algorithm is run to maximize the mean torque while minimizing the torque ripple. Evaluations are performed by a 2D nonlinear finite element magnetic model. The obtained Pareto fronts show that the optimization is able to reduce the torque ripple down to about 4% for all the types, with little impact on the mean torque. The round FB have the highest mean torque and a better convergence speed than rectangular and hyperbolic FB, whereas the Joukowski FB, with half as many parameters, reaches 98% of the round FB torque. Also, the proposed parameterization reaches the optimization convergence up to 3.5 times faster than a conventional parameterization, for all the FB types.

I. INTRODUCTION

Synchronous reluctance motors (SynRM) have gained interest over the years. Their low manufacturing cost and high efficiency make them an interesting alternative to induction motors. However, their power factor remains low and they can suffer from high torque ripple. Therefore, a meticulous design of the rotor is mandatory. In order to keep the number of design parameters limited, several flux barriers (FB) types are proposed in the literature. The most investigated ones are the rectangular FB [1], the round FB [2], and the Joukowski FB [3].

The choice of the flux barriers type is an important step in the design of SynRM. This decision is made prior to the parameterization of the rotor and the development of numerical models, that will then be interfaced with an optimizer. Therefore, analyzing the performances of another flux barriers type requires to adapt the parameterization, the models, and the interface with the optimizer. This time-consuming work is rarely performed, which arbitrarily freezes the flux barriers type at the early stages of the design phase. However, the impact of the flux barriers type on the performances of the machine is still poorly investigated. The only study found in the literature is [4], where rectangular and round FB have been

compared. The current study extends this comparison by considering, in addition to rectangular and round FB, hyperbolic and Joukowski FB. A multi-objective genetic algorithm is run to maximize the mean torque while minimizing the torque ripple. The comparison is performed based on the Pareto fronts generated by the optimization algorithm.

Also, there are several ways to parameterize the flux barriers. The geometric constraints can be obeyed either by explicitly writing the expression of these constraints, or by providing a parameterization that implicitly complies with these constraints. Although the different parameterizations lead to the same geometry by the end of the design process, this paper shows that the convergence speed is greatly impacted by the parameterization. The hypervolume indicator is used to compare the convergence speed of a direct parameterization, where the design parameters are the positions and thicknesses of the flux barriers, and an indirect parameterization, that simplifies the geometric constraints.

II. FLUX BARRIER TYPES

The different flux barrier types investigated in this paper are represented in Fig. 1. The rectangular FB (a) have straight lines, which are interesting to position permanent magnets, used in permanent magnet assisted synchronous reluctance motors (PMASynRM). The round (b) and hyperbolic (c) FB are defined by conics, the former using circles, the latter using hyperbolas. Finally, the Joukowski FB (d) follow the natural flux lines in a solid rotor. These flux lines are approximated by using the Joukowski airfoil potential function [5]:

$$r(\theta) = R_{in} \cdot \sqrt[p]{\frac{C + \sqrt{C^2 + 4 \sin^2(p\theta)}}{2 \sin(p\theta)}} \quad (1)$$

with R_{in} the inner radius of the rotor, p the number of pole pairs, and C a constant which is a function of the cylindrical point coordinates (r, θ) that the curve is passing through:

$$C = \frac{\sin(p\theta) \cdot \left[\left(\frac{r}{R_{in}} \right)^{2p} - 1 \right]}{\left(\frac{r}{R_{in}} \right)^p}. \quad (2)$$

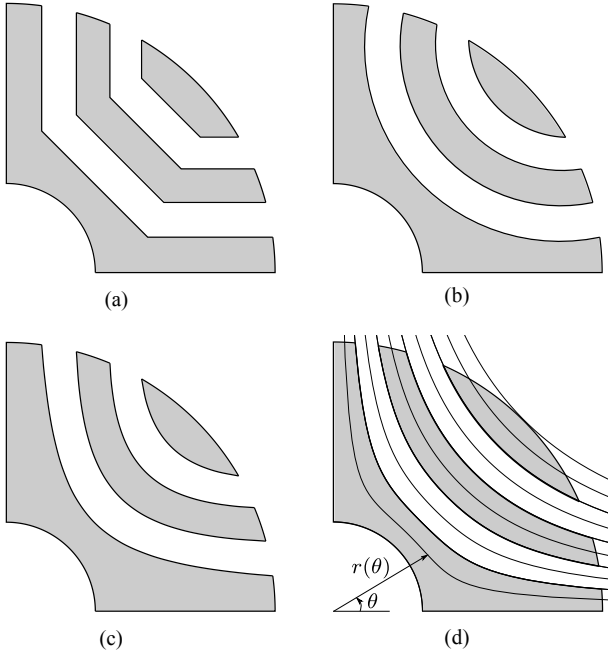


Fig. 1. Flux barriers types. (a) Rectangular. (b) Round. (c) Hyperbolic. (d) Joukowski.

III. PARAMETERIZATION

The flux barriers have to be positioned in the rotor yoke, regardless of their type. With an unconstrained design space, the optimizer might test several sets of parameters that could result in an overlap between flux barriers. This can lead to erroneous evaluation of the performances of the machine and impacts negatively the convergence of the optimization. There are two ways to prevent this problem from happening:

- By explicitly constraining the optimization problem to parameters that satisfy the non-overlapping constraints. Depending on the parameterization, these non-overlapping constraints can be difficult to formulate or to comply with.
- By using an indirect parameterization that implicitly obeys the non-overlapping constraints. This leads to a more robust design space, but it also shapes the optimization problem differently, which can become more prone to local minima.

Both ways are implemented, described and compared.

A. Direct parameterization

The positions and thicknesses of the flux barriers are the design parameters, as shown in Fig. 2. The parameters d_i and t_i correspond to the radial position and thickness of the flux barrier i . Similarly, the parameters α_i and $\Delta\alpha_i$ correspond to the angular position and thickness of the tip of the flux barrier i . Each flux barrier is numbered starting from the center of the rotor. The non-overlapping constraints on the radial direction can be explicitly written:

$$\begin{cases} d_i + t_i < d_{i+1} & \text{if } i \neq n \\ d_i + t_i < R_{out} & \text{otherwise} \end{cases} \quad (3)$$

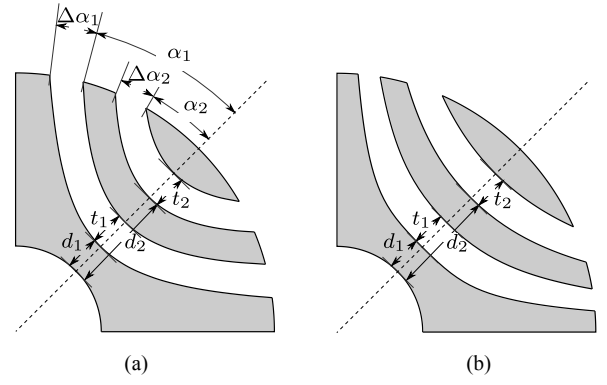


Fig. 2. Direct parameterization for (a) hyperbolic FB (also applicable to rectangular and round FB). (b) Joukowski FB.

with R_{out} the outer radius of the rotor and n the total number of flux barriers. Similarly, the non-overlapping constraints on the tangential direction are:

$$\begin{cases} \alpha_i + \Delta\alpha_i < \frac{1}{2} \cdot \pi/p & \text{if } i = 1 \\ \alpha_i + \Delta\alpha_i < \alpha_{i-1} & \text{otherwise.} \end{cases} \quad (4)$$

In addition to the non-overlapping constraints (3) and (4), all the parameters d_i , t_i , α_i , and $\Delta\alpha_i$ must be strictly positive. These additional constraints are implicitly taken into account when defining the bounds of the optimization variables.

The above-mentioned parameters, d_i , t_i , α_i , and $\Delta\alpha_i$, define two points in the radial direction and two points in the tangential direction, per flux barrier. These points determine the inner and outer boundaries of the flux barrier i at the center and at the tip. Assuming a symmetric rotor, there only exists a unique possibility to construct a rectangular, a round, or a hyperbolic flux barrier passing through these points.

When considering the Joukowski flux barrier, the points located at the center of the flux barriers are sufficient to determine two flux lines along which the flux barrier is carved. As a consequence, the angular parameters α and $\Delta\alpha$ and their associated constraint (4) do not apply to Joukowski flux barriers. Ergo, the Joukowski type requires only 2 parameters by flux barrier (d_i and t_i), which is half as many parameters as the other types (d_i , t_i , α_i , and $\Delta\alpha_i$). Reducing the number of parameters benefits the convergence speed of the optimization.

B. Indirect parameterization

In this parameterization, the positions and thicknesses of the flux barriers are determined indirectly with a set of virtual springs that mechanically repel constructive points that cannot meet (Fig. 3). The stiffnesses K_i of these springs are the new design parameters, which yields a parameter space with no other internal constraint than the positiveness of the stiffnesses. Another advantage is that all parameters have the same nature (whereas geometrical parameters can be lengths or angles), which basically acts as an implicit normalization of the design space.

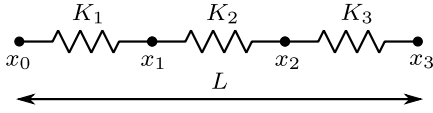


Fig. 3. Spring-based approach.

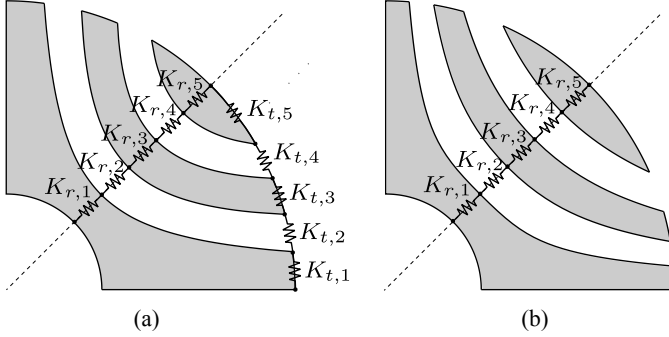


Fig. 4. indirect parameterization for (a) hyperbolic FB (also applicable to rectangular and round FB). (b) Joukowski FB.

The stiffness network can be solved explicitly:

$$x_i = x_{i-1} + \frac{K_i}{\sum_{k=1}^m K_k} L \quad (5)$$

with x the position of the point, K the stiffness of the spring, L the combined length of the springs, and m the number of springs. As a consequence, it is not possible to modify the position of a single point without modifying all the parameters together. This shapes the optimization problem differently, which has an impact on the optimization convergence.

This spring-based parameterization is applied to the different flux barriers profiles in Fig. 4. Each set of springs positions points in one direction, radially or tangentially, that define the inner and outer boundaries of the flux barriers, at the center and at the tip. By assuming a symmetric rotor, the flux barriers can then be constructed in a unique way. This way of constructing the geometry is the same as in the direct parameterization, except that the position of the points are determined indirectly by solving stiffness networks.

As it has been previously discussed, the points located on the center of the flux barriers are sufficient to define a Joukowski flux barrier. As a consequence, this type only requires the radial set of springs, while the other types (rectangular, round, and hyperbolic) require both the radial and the tangential sets.

IV. OPTIMIZATION

A NSGA-II [6] algorithm is run to maximize the mean torque and to minimize the torque ripple. These quantities are evaluated by a quasi-static 2D FEM nonlinear magnetic model, which uses the nonlinear solver GetDP [7].

The search space is kept as wide as possible. The design parameters boundaries are summarized for both the direct and the indirect parameterizations in Table I and Table II. The

TABLE I
SEARCH SPACE BOUNDARIES FOR THE DIRECT PARAMETERIZATION
($i = 1, 2, \dots, n$)

Parameter	Lower bound	Upper bound	Units
d_i	0	100	mm
t_i	0	40	mm
α_i	0	$\pi/4$	rad
$\Delta\alpha_i$	0	$\pi/12$	rad

TABLE II
SEARCH SPACE BOUNDARIES FOR THE INDIRECT PARAMETERIZATION
($i = 1, 2, \dots, 2n + 1$)

Parameter	Lower bound	Upper bound	Units
$K_{r,i}$	0.1	10	/
$K_{t,i}$	0.1	10	/

indirect and direct parameterizations have $4n+2$ and $4n$ design parameters, respectively ($2n+1$ and $2n$ in the special case of Joukowski FB). The extra design parameters of the indirect parameterization are not required to cover the entire design space, the stiffness of a spring from each stiffness networks (e.g., $K_{r,2n+1}$ and $K_{t,2n+1}$) could be arbitrarily frozen during the optimization process. Nonetheless, the optimizations systematically got stucked in local minima when doing so. The optimization convergence issues disappeared when keeping these extra stiffnesses in the design space.

The external dimensions of the rotor are kept constant, with a 50 mm inner radius and a 150 mm outer radius. The number of flux barriers n is set to four. The motor has two pole pairs, an airgap of 1.5 mm, and an outer radius of 250 mm. The 48 slots stator is fed by a three-phase sinusoidal current, which has a peak current density of 8.5 A/mm². This working point leads to a high level of magnetic saturation in the rotor and stator yokes. The current angle is adjusted to 60° to remain close to the maximum torque per ampere control strategy.

V. RESULTS

The hypervolume indicator [8] is used to compare the optimization convergence of the direct and indirect parameterizations. This single scalar metric, illustrated in Fig. 5, measures both the proximity of the Pareto front to the true Pareto front and the spread of solutions across the objective space. The hypervolume is maximized if and only if the set of solutions contains all true Pareto optimal points [9].

The hypervolume indicator is computed on the successive Pareto fronts obtained at each generation of the genetic algorithm. The results are visible on Fig. 6. The proposed parameterization, represented with the red dashed line, persistently reaches the convergence faster than the direct parameterization, represented with the blue solid line. The converged value is identical for both parameterizations. Also, the Joukowski flux barriers (d) reaches the convergence faster

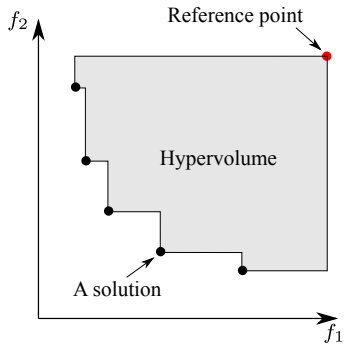


Fig. 5. Hypervolume for two objectives being minimized.

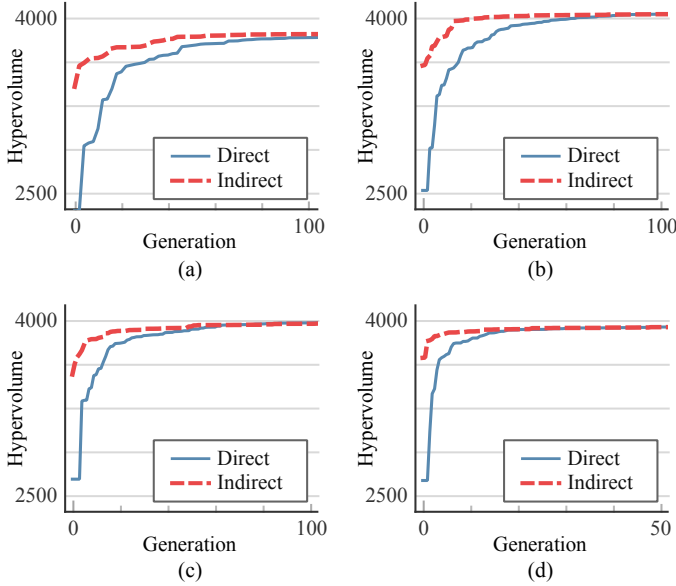


Fig. 6. Evolution of the hypervolume over the generations, for both the direct and indirect parameterizations. (a) Rectangular. (b) Round. (c) Hyperbolic. (d) Joukowski.

than the rectangular (a), round (b), and hyperbolic (c) flux barriers. These observations are quantified in Table III.

The maximum value reached by the hypervolume indicator is not the same for the different flux barriers, which means that the Pareto fronts are not identical either. These Pareto fronts are visible in Fig. 7. The fronts are steep, a small decrease of the mean torque drastically lowers the torque ripple. All the types succeed to reach a torque ripple as low

TABLE III
NUMBER OF GENERATIONS BEFORE REACHING 98% OF THE
HYPERVOLUME CONVERGENCE VALUE, DEPENDING ON THE FLUX
BARRIER TYPE AND THE PARAMETERIZATION.

	Direct parameterization	Indirect parameterization
Rectangular	70	33
Round	46	13
Hyperbolic	43	16
Joukowski	27	8

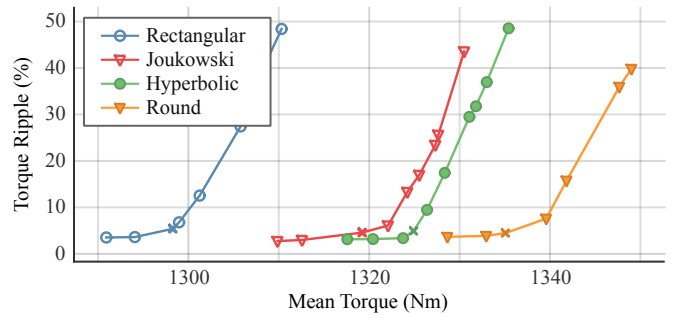


Fig. 7. Pareto fronts for the different flux barriers types.

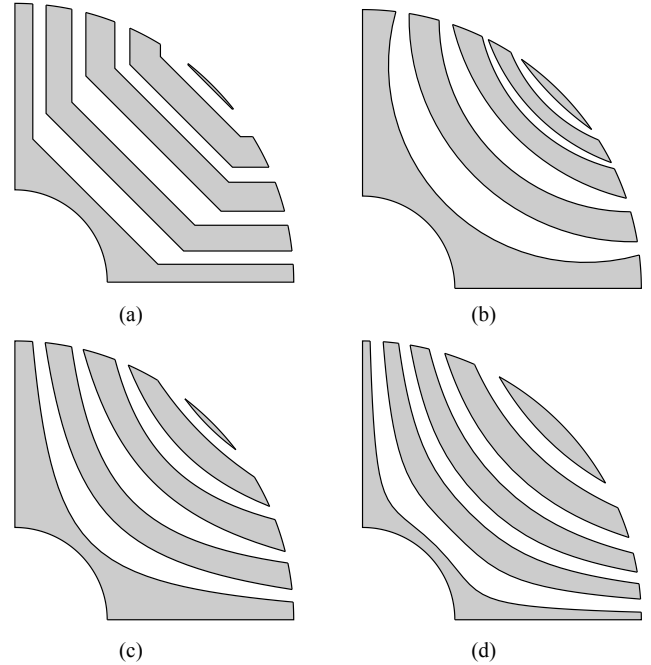


Fig. 8. Geometries selected from the Pareto fronts. (a) Rectangular. (b) Round. (c) Hyperbolic. (d) Joukowski.

as 4%. When considering the mean torque, the round flux barriers outperforms all the other types. The least performing type is the rectangular flux barriers. Nonetheless, less than 3% variation on the mean torque is observed between these two types. This difference is reduced to less than 1.5% when comparing round FB to Joukowski or hyperbolic FB.

The points marked with an 'x' in Fig. 7 represent a decent trade-off between the mean torque and the torque ripple, which remains close to 5%. The geometries corresponding to these points are shown in Fig. 8.

VI. CONCLUSION

This paper has brought a comparison between the rectangular, hyperbolic, round, and Joukowski flux barriers. Two different parameterizations have been described and implemented. In the direct parameterization, the position and thicknesses of the flux barriers are directly the design parameters of the rotor. This parameterization includes several geometric constraints,

that can be simplified by using an indirect parameterization. This last parameterization determines the position and thicknesses of the flux barriers indirectly by solving stiffness networks.

The results show that the flux barriers type has a limited influence on the mean torque and nearly no impact on the torque ripple. However, the FB type and its parameterization affects the convergence speed of the optimization significantly. The best convergence speed is obtained by the Joukowski FB, which have similar mean torque to hyperbolic FB. The round FB have the highest mean torque and come just next to the Joukowski FB in terms of convergence speed. Finally, the rectangular FB have the lowest mean torque and a lower convergence speed than the other flux barrier types. In all these cases, the spring parameterization proposed in this paper considerably speeds up the optimization process.

REFERENCES

- [1] R. Moghaddam and F. Gyllensten, "Novel High-Performance SynRM Design Method: An Easy Approach for A Complicated Rotor Topology," *IEEE Transactions on Industrial Electronics*, vol. 61, no. 9, pp. 5058–5065, Sep. 2014.
- [2] A. Tassarolo, "Modeling and Analysis of Synchronous Reluctance Machines With Circular Flux Barriers Through Conformal Mapping," *IEEE Transactions on Magnetics*, vol. 51, no. 4, pp. 1–11, April 2015.
- [3] M. Palmieri, M. Perta, F. Cupertino, and G. Pellegrino, "Effect of the numbers of slots and barriers on the optimal design of synchronous reluctance machines," in *2014 International Conference on Optimization of Electrical and Electronic Equipment (OPTIM)*, May 2014, pp. 260–267.
- [4] G. Pellegrino, F. Cupertino, and C. Gerada, "Automatic Design of Synchronous Reluctance Motors Focusing on Barrier Shape Optimization," *IEEE Transactions on Industry Applications*, vol. 51, no. 2, pp. 1465–1474, March 2015.
- [5] J. H. Mathews and R. W. Howell, *Complex Analysis for mathematics and engineering*, 4th ed. Jones and Bartlett Publishers, 2001.
- [6] K. Deb, A. Pratap, S. Agarwal, and T. Meyarivan, "A fast and elitist multiobjective genetic algorithm: NSGA-II," *IEEE Transactions on Evolutionary Computation*, vol. 6, no. 2, pp. 182–197, April 2002.
- [7] P. Dular, C. Geuzaine, F. Henrotte, and W. Legros, "A general environment for the treatment of discrete problems and its application to the finite element method," *IEEE Transactions on Magnetics*, vol. 34, no. 5, pp. 3395–3398, Sep. 1998.
- [8] L. While, P. Hingston, L. Barone, and S. Huband, "A faster algorithm for calculating hypervolume," *IEEE Transactions on Evolutionary Computation*, vol. 10, no. 1, pp. 29–38, Feb 2006.
- [9] M. Fleischer, "The measure of pareto optima applications to multi-objective metaheuristics," in *Evolutionary Multi-Criterion Optimization*, C. M. Fonseca, P. J. Fleming, E. Zitzler, L. Thiele, and K. Deb, Eds. Berlin, Heidelberg: Springer Berlin Heidelberg, 2003, pp. 519–533.